# You Only Look at Screens: Multimodal Chain-of-Action Agents

**Anonymous ACL submission**

## Abstract

Autonomous graphical user interface (GUI) agents aim to facilitate task automation by interacting with the user interface without manual intervention. Recent studies have investigated eliciting the capabilities of large language models (LLMs) for effective engagement in diverse environments. To align with the input-output requirement of LLMs, most existing approaches are developed under a sandbox setting where they rely on external tools and application-specific APIs to parse the environment into textual elements and interpret the predicted actions. Consequently, those approaches often grapple with inference inefficiency and error propagation risks. To mitigate the challenges, we introduce Auto-GUI, a multimodal solution that directly interacts with the interface, bypassing the need for environment parsing or reliance on application-dependent APIs. Moreover, we propose a chain-of-action technique—leveraging a series of intermediate previous action histories and future action plans—to help the agent decide what action to execute. We evaluate our approach on a new device-control benchmark AITW with $30K$ unique instructions, spanning multi-step tasks such as application operation, web searching, and web shopping. Experimental results show that Auto-GUI achieves state-of-the-art performance with an action type prediction accuracy of 90% and an overall action success rate of 74%. Code is publicly available at `Anonymous`.

## 1 Introduction

Building intelligent autonomous agents that are capable of task planning, decision making, and action execution in a particular environment is a long-standing goal of artificial intelligence (AI) (Searle, 1969; Wooldridge and Jennings, 1995; Maes, 1995; Hendler, 1999). The advent of large language models (LLMs) (Brown et al., 2020; Chowdhery et al., 2022; OpenAI, 2023) has flourished promising opportunities for developing autonomous agents to assist users in completing tasks in distinct environments such as operation systems, specific applications, and web browsers (Adept, 2022; Rawles et al., 2023; Liu et al., 2023; Zhou et al., 2023; Wang et al., 2023c; Koh et al., 2024; Gao et al., 2023; Yang et al., 2023).

Recent studies have explored prompt engineering (Richards, 2023; Nakajima, 2023; Reworkd, 2023; Sumers et al., 2023; Liu et al., 2023) and fine-tuning techniques (Rawles et al., 2023; Wen et al., 2023; Sun et al., 2022) to elicit the capability of language models to execute actions in interactive environments. However, there are at least two major challenges that have limited real-world applications of autonomous agents.

First, existing approaches commonly rely on external tools such as optical character recognition (OCR) and icon detectors (Zhang et al., 2021; Sunkara et al., 2022) to parse the environment into textual elements (e.g., HTML layouts) as inputs to a language model (Figure 1(a)) (Rawles et al., 2023). On the one hand, the parsed elements generate lengthy inputs, thus leading to inference inefficiency. Since computational latency is a key measure in deployment, using lengthy inputs would increase inference cost and may even exceed the input length limit of the language model. On the other hand, parsing the visual environment into textual elements may also be prone to error propagation or information loss because parsing mistakes are inevitable using external tools.

Second, most existing approaches are under the sand-box setting that requires accessing internal APIs to interact with the environment (Zhou et al., 2023; Gur et al., 2023), e.g., using a JavaScript element selection on a webpage or a Python interpreter to execute actions. However in practice, the API interface is often inaccessible in third-party applications (Apps).

These challenges have motivated more advanced techniques that are capable of *first principles think-*

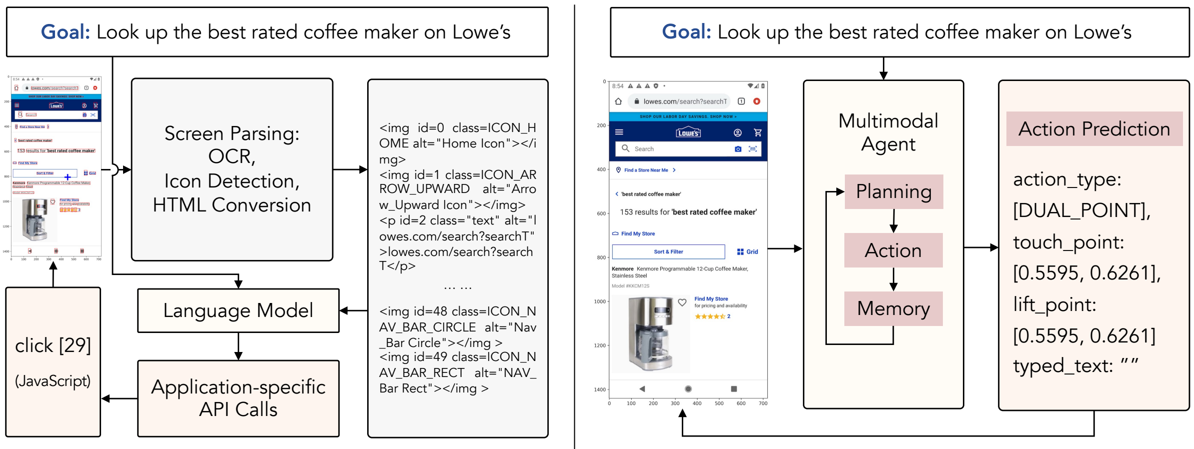
Goal: Look up the best rated coffee maker on Lowe's
Screen Parsing: OCR, Icon Detection, HTML Conversion
Language Model
Application-specific API Calls
click [29]
(JavaScript)
Goal: Look up the best rated coffee maker on Lowe's
Multimodal Agent
Planning
Action
Memory
Action Prediction

```
<img id=0 class=ICON_HOME alt="Home Icon"></img>
<img id=1 class=ICON_ARROW_UPWARD alt="Arrow_Upward Icon"></img>
<p id=2 class="text" alt="lowes.com/search?searchT">lowes.com/search?searchT</p>
... ...
<img id=48 class=ICON_NAV_BAR_CIRCLE alt="Nav_Bar Circle"></img >
<img id=49 class=ICON_NAV_BAR_RECT alt="NAV_Bar Rect"></img >
```

action_type: [DUAL_POINT],
touch_point: [0.5595, 0.6261],
lift_point: [0.5595, 0.6261]
typed_text: “”

(a) Sandbox Paradigm

(b) First Principles Thinking Paradigm

Figure 1: Comparison of GUI agent paradigms. The sandbox paradigm depends on the intermediate transformation between environments and agents, i.e., needing access to intermediate environment parsing or interval application-dependent APIs. In contrast, our first principles thinking paradigm allows direct interactions on the screen without intermediate transformation. Details of the action types and action points are presented in Section 3.3.

*ing* (Aristotle; Irwin, 1989)—allowing direct interactions on the screen without needing access to intermediate environment parsing or interval application-dependent APIs (Figure 1(b)). To address the challenges, we introduce **Auto-GUI**, a multimodal approach that directly interacts with the graphical user interfaces (GUIs). To further strengthen the agent's action prediction capability, we propose a novel **chain-of-action** technique, where a chain of action is a series of intermediate previous action histories and future action plans that lead to action prediction.

We evaluate Auto-GUI on a new device-control benchmark AITW (Rawles et al., 2023) with 30$K$ unique instructions, spanning multi-step tasks of application operation, web searching, and web shopping. Experimental results show that Auto-GUI achieves state-of-the-art performance with an action type prediction accuracy of 90% and an action success rate of 74%.

In summary, our work makes the following technical contributions:

(i) We introduce Auto-GUI, a multimodal agent for autonomous GUI control that can directly interact with the screens, thus circumventing the constraints of environment parsing and application-specific API access.

(ii) We propose a chain-of-action technique that leverages the previously executed actions and future action plans to help the agent decide what action to execute at each step.

(iii) Auto-GUI achieves state-of-the-art performance with an action type prediction accuracy of 90% and an action success rate of 74%. Notably, Auto-GUI can infer an action as fast as within less than one second.

## 2 Related Work

Our work falls into the field of language agents. This section will first review the recent progress in building language agents and then discuss the approaches to conduct user interface control with language agents.

### 2.1 Language Agents

Language agents refer to those agents that can follow user instructions and interact with environments to complete tasks. Such agents expand the landscape of language models to compete in specific fields, including application operation, web searching, and web shopping. There are two popular types of language agents, autonomous agents and communicative agents. Autonomous agents aim to assist humans to achieve specific goals in the real world. Typical examples of autonomous agents are AutoGPT (Richards, 2023), BabyAGI (Nakajima, 2023), and AgentGPT (Reworkd, 2023). In contrast, communicative agents are personalized and socialized agents (Park et al., 2023; Wang et al., 2023b; Zhu et al., 2023; Hong et al., 2023a) with human behaviors that can communicate and collaborate with each other. They are often deployed in immersive environments.

Inspired by the potential in real-world applications, this work focuses on autonomous agents, especially those working in mobile devices. We aim

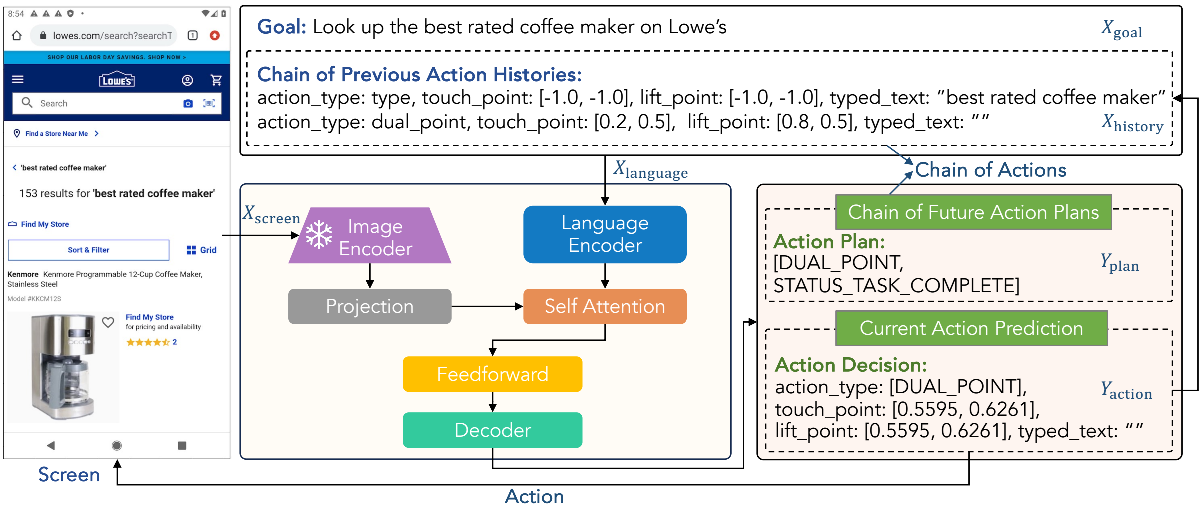

Goal: Look up the best rated coffee maker on Lowe's $X_{\text{goal}}$

Chain of Previous Action Histories:
action_type: type, touch_point: [-1.0, -1.0], lift_point: [-1.0, -1.0], typed_text: "best rated coffee maker"
action_type: dual_point, touch_point: [0.2, 0.5], lift_point: [0.8, 0.5], typed_text: "" $X_{\text{history}}$

Action Plan:
[DUAL_POINT,
STATUS_TASK_COMPLETE] $Y_{\text{plan}}$

Action Decision:
action_type: [DUAL_POINT],
touch_point: [0.5595, 0.6261],
lift_point: [0.5595, 0.6261], typed_text: "" $Y_{\text{action}}$

Figure 2: Model architecture of Auto-GUI. A chain of action consists of a chain of previous action histories $X_{\text{history}}$ and a chain of future action plans $Y_{\text{plan}}$ in the illustration.

to assist users by completing multi-step tasks (e.g., manipulating Apps, web shopping, and question answering) without any manual intervention. Given a user instruction in natural language, the agent is required to interpret the instruction and execute actions by directly controlling its user interface. Due to the requirement in real-world applications, the agent is expected to be both effective and efficient.

### 2.2 GUI Control with Natural Language

Recently, LLMs have shown promise in building autonomous GUI agents with abilities of instruction following (Sanh et al., 2022; Taori et al., 2023b; Chiang et al., 2023) and chain-of-thought (CoT) prompting (Nye et al., 2022; Wei et al., 2022). Especially, CoT prompting (Wei et al., 2022; Kojima et al., 2022; Zhang et al., 2023a) elicit LLMs' capacities of step-by-step planning, decision making, and action execution. Those capacities have been shown to be effective in GUI control tasks (Rawles et al., 2023).

However, the task environments are GUIs instead of natural language that LLMs can process directly. Therefore, the GUI states and actions are required to be converted to textual formats to be applicable to LLMs. For example, it is feasible to parse the GUI screens by icon recognition and OCR (Zhang et al., 2021; Sunkara et al., 2022; Song et al., 2023) and organize the parsed elements into HTML layouts. As a compromise, existing approaches are restricted in a sandbox setting where they rely on external tools (Rawles et al., 2023; Wen et al., 2023) and application-specific APIs (Zhou et al., 2023; Gur et al., 2023) for environment parsing and action interpretation; thus, commonly suffer from inference inefficiency and error propagation. Although there are studies that have considered multimodal architecture for processing inputs in different modalities (Sun et al., 2022; Yan et al., 2023), those studies still rely on fine-grained environment parsing to ensure competitive performance. As GUI tasks have shown prerequisites to fine-grained grounding to the GUI contents, more recent concurrent studies (Cheng et al., 2024; Hong et al., 2023b) have explored GUI grounding pretraining to improve the agent's performance.

In contrast to the studies above, this work is established upon first principles thinking, which directly reads GUI without additional environment parsing and provides the action (e.g., action type, gesture coordinate, and typed text) that can be efficiently executed without needing any extra APIs.

## 3 Methodology

In this section, we will first introduce the basic concepts for the GUI control task and then describe the design of our proposed Auto-GUI framework.

### 3.1 Problem Formalization

Given a user instruction (also known as a *goal*), the agent needs to complete the task with multiple steps of interactions. The entire process is called an *episode*, which is composed of a series of *screens*. For each step in the episode, the agent will be provided with a screenshot, and the agent is required to predict the action until the task is complete. Detailed examples can be found in Appendix A.1.

### 3.2 Framework Overview

Auto-GUI is a multimodal agent that decides what action to take given the input screenshot and a user instruction. To empower the agent's decision making capability, we introduce a chain-of-action approach by leveraging a series of intermediate previous action histories and future action plans to predict actions.

The model architecture of Auto-GUI is illustrated in Figure 2. On a high level, Auto-GUI consists of three stages. First, we acquire encoded features from both vision and language inputs. Specifically, the vision input, i.e., a screenshot, is encoded by a frozen vision encoder. Meanwhile, the language input, consisting of the goal and a chain of previous action histories—each history contains a tuple {action type, touch point, lift point, and typed text}, is encoded by a language encoder. Second, the encoded vision and language representations are integrated by a self-attention module. Third, the fused representation is fed to the decoder to generate a chain of future action plans (i.e., action types to execute in future steps) followed by action prediction. A chain of action consists of two parts in the procedure above: a chain of previous action histories on the input side and a chain of future action plans on the output side. In the following, we describe the entire procedure in detail.

**Encoding** Suppose that an episode consists of $k$ steps of interactions. Given a screenshot $X_{\text{screen}} \in \mathbb{R}^{h \times w \times 3}$ with height $h$ and width $w$ at step $t \in [1, k]$, we first feed it to a frozen image encoder (e.g., BLIP-2 (Li et al., 2023)) and extract vision features $H_{\text{screen}} \in \mathbb{R}^{1 \times d_s}$ where $d_s$ is the dimension of the vision features. Additionally, we leverage a language encoder to extract the language features $H_{\text{language}} \in \mathbb{R}^{n \times d_l}$ of the input goal $X_{\text{goal}}$ where $n$ is the number of tokens and $d_l$ is the dimension of the language features. If $t > 1$, there will be a chain-of-action history already executed before step $t$. We denote the chain of action histories as $X_{\text{history}} = [m_1, \ldots, m_t]$ where $m_i$ contains a tuple of action type, touch point, lift point, and typed text. Otherwise, if $t = 1$, $X_{\text{history}}$ will be set empty:

$$X_{\text{history}} = \begin{cases} [m_1, \ldots, m_t], & \text{if } t > 1 \\ \text{<empty>}, & \text{otherwise} \end{cases} \quad (1)$$

We concatenate $X_{\text{goal}}$ and $X_{\text{history}}$ as the input to the language encoder: $X_{\text{language}} = \{X_{\text{goal}}, X_{\text{history}}\}$.

Then, we obtain the encoded representations of the vision and language inputs as follows:

$$\begin{aligned} H_{\text{screen}} &= \text{VisionExtractor}(X_{\text{screen}}), & (2) \\ H'_{\text{screen}} &= W H_{\text{screen}}, & (3) \\ H_{\text{language}} &= \text{LanguageEncoder}(X_{\text{language}}), & (4) \end{aligned}$$

where $W$ is a trainable projection matrix to convert $H_{\text{screen}}$ into the same dimensionality as $H_{\text{language}}$.

**Interaction** We correlate $H'_{\text{screen}}$ and $H_{\text{language}}$ with a single-head self-attention network (Vaswani et al., 2017), where the query ($Q$), key ($K$), and value ($V$) are $H_{\text{language}}$, $H'_{\text{screen}}$, and $H'_{\text{screen}}$, respectively. The attention output $H^{\text{attn}}_{\text{screen}} \in \mathbb{R}^{n \times d}$ is defined as: $H^{\text{attn}}_{\text{screen}} = \text{Softmax}(\frac{QK^\top}{\sqrt{d_k}})V$, where $d_k$ is the same as the dimension of $H_{\text{language}}$ because a single head is used.

Then, a gated fusion is adopted following prior studies (Zhang et al., 2020; Wu et al., 2021; Zhang et al., 2023b) to fuse $H_{\text{language}}$ and $H^{\text{attn}}_{\text{screen}}$. We have the fused output $H_{\text{fuse}} \in \mathbb{R}^{n \times d}$ by:

$$\begin{aligned} \lambda &= \text{Sigmoid}(W_l H_{\text{language}} + W_v H^{\text{attn}}_{\text{vision}}), & (5) \\ H_{\text{fuse}} &= (1 - \lambda) \cdot H_{\text{language}} + \lambda \cdot H^{\text{attn}}_{\text{vision}}, & (6) \end{aligned}$$

where $W_l$ and $W_v$ are learnable parameters.

**Decoding** The fused representation $H_{\text{fuse}}$ is fed to a Transformer decoder to generate the target predictions in a string format. The target predictions consist of a chain of future action plans $Y_{\text{plan}}$ and the current action prediction $Y_{\text{action}}$ separated by specific prompts: {Action Plan: $Y_{\text{plan}}$, Action Decision: $Y_{\text{action}}$}. Concretely, $Y_{\text{plan}}$ is a chain of action types to execute in future steps: $Y_{\text{plan}}$ = [action_type$_t$, ..., action_type$_k$]. $Y_{\text{action}}$ contains four components: $Y_{\text{action}}$ = {"action_type": <action_type>, "touch_point": <touch_point>, "lift_point": <lift_point>, "typed_text": <typed_text>}. These four components will be explained as follows.

### 3.3 Coordinate Normalization

Recall that a target action consists of four components: action type, touch point, lift point, and typed text. We consider six action types: *dual-point gesture*, *type*, *go_back*, *go_home*, *enter*, and *status_complete*. A dual-point gesture comprises a touch point and a lift point with $[y, x]$ coordinates. The gesture actions ensure a flexible action space and can represent clicks and scrolls at arbitrary locations. For example, a gesture action {“touch_point”: [0.7761, 0.7089], “lift_point”: [0.7761, 0.7089]} means clicking at the coordinate [0.7761, 0.7089], while a gesture action {“touch_point”: [0.1898, 0.4477], “lift_point”: [0.8242, 0.4077]} means scrolling down. A type action means typing a text and the text is placed in the <typed_text> field. The other action types, i.e., go_back, go_home, enter, and status_complete are system actions, whose corresponding <touch_point>, <lift_point> fields are filled with -1, and the <typed_text> is empty.

We observe that high-precision coordinates are not necessary for representing a click or scroll action. Therefore, we apply normalized values of the coordinates, which helps accelerate convergence and mitigate the ambiguity of coordinates. The normalization is applied to click and scroll actions. For click actions, we keep four decimal places. For scroll actions, we first determine the scroll direction with the touch and lift points. Then, we transform the touch and lift points into fixed directional coordinates as follows: “up”: {[0.8, 0.5], [0.2, 0.5]}, “down”: {[0.2, 0.5], [0.8, 0.5]}, “left”: {[0.5, 0.8], [0.5, 0.2]}, “right”: {[0.5, 0.2], [0.5, 0.8]}, where {[·], [·]} consists of the touch point and lift point in the first [·] and second [·]. We provide examples of target actions in Appendix B.1.

## 4 Experiments

### 4.1 Dataset

We use the AITW benchmark dataset (Rawles et al., 2023). AITW is a large-scale GUI control benchmark dataset containing natural language instructions, screenshots, and actions. There are 715$K$ episodes spanning 30$K$ unique instructions, covering diverse multi-step tasks such as application operation, web searching, and web shopping, on over 350 Apps and websites. This dataset covers various device types and operation systems in varying screen resolutions to ensure generality. There are five subsets in the benchmark dataset, namely, General, Install, GoogleApps, Single, and WebShopping. The details of the subsets and data statistics are presented in Appendix A.2.

### 4.2 Baselines

We adopt three types of baselines, allowing for a comprehensive comparison with our approach. The baselines encompass the in-context earning (ICL) and fine-tuning paradigms. They are based on various backbone models of different sizes.

(i) In-context Learning LLMs. Few-shot PaLM 2, ChatGPT (turbo-3.5) are adopted. Following prior studies (Rawles et al., 2023; Wang et al., 2023a), we feed the LLM a textual description of the screen and a user instruction. The screen is formatted as an HTML syntax, providing the information of GUI elements derived from OCR detection and icon detection from external tools (Rawles et al., 2023). The model is required to predict an action among pre-defined actions. In addition, we report the results of the multimodal GPT-4V by taking the vision image and action history as the input based on Yan et al. (2023).

(ii) Fine-tuned LLMs. We adopt Llama-2-7B (Touvron et al., 2023) as the baseline and fine-tune it with LoRA. We feed the model with the user instruction and the screen descriptions in HTML syntax (the same as in-context learning LLMs). The model is expected to predict the action in the same output format as in-context learning LLMs.

(iii) Specialized GUI Agent. We adopted the Behavioural Cloning (BC) agent, which reported the state-of-the-art performance in Rawles et al. (2023). BC is a Transformer-based architecture that takes a task instruction, the current screen, and a stacked history of screen observations and actions as input. All the embedded representations are fused to predict the action by a decoder. There are two BC variants, BC-single and BC-history, depending on whether the model takes the screen-action history as input.

More detailed implementation of the baselines can be found in Appendix B.2.

### 4.3 Evaluation Measures

We compute the screen-wise action matching score as the main evaluation measure, defined as the number of correct actions divided by the episode length. A predicted action is considered correct if the action type and dual-point gesture match the gold ones. As we described in Section 3.3, the gesture actions can represent the click actions and scroll actions at arbitrary locations. Following Rawles et al. (2023), a click action is considered correct if its touch point and lift point fall within a 14% screen distance from the gold gestures or occur within the same detected bounding box with the gold gestures. A scroll action is considered correct if it has the same scroll axis as the gold gesture.

The screen-wise action matching score has been shown to correlate with the task complete score estimated by human evaluations (Rawles et al., 2023)

| Model | Unified | w/o Anno. | Overall | General | Install | GoogleApps | Single | WebShopping |
|---|---|---|---|---|---|---|---|---|
| PaLM 2-CoT | ✓ | ✗ | 39.6 | - | - | - | - | |
| ChatGPT-CoT | ✓ | ✗ | 7.72 | 5.93 | 4.38 | 10.47 | 9.39 | 8.42 |
| GPT-4V | ✓ | ✗ | 52.96 | 43.01 | 46.14 | 49.18 | 78.29 | 48.18 |
| Fine-tuned Llama 2 | ✗ | ✗ | 28.40 | 28.56 | 35.18 | 30.99 | 27.35 | 19.92 |
| BC-single | ✗ | ✗ | 68.7 | - | - | - | - | |
| BC-history | ✗ | ✗ | 73.1 | 63.7 | 77.5 | 75.7 | 80.3 | 68.5 |
| Auto-GUI$_{\text{separate}}$ | ✗ | ✓ | 74.07 | 65.94 | **77.62** | **76.45** | 81.39 | 69.72 |
| Auto-GUI$_{\text{unified}}$ | ✓ | ✓ | **74.27** | **68.24** | 76.89 | 71.37 | **84.58** | **70.26** |

Table 1: Main results (%). Segment 1: specialized agent baselines; Segment 2: in-context learning LLM baselines; Segment 3: fine-tuned Llama 2 baseline; Segment 4: our Auto-GUI results. Prior published best results are marked with an underline. "Unified" means a general model that can work across subsets. "w/o Anno." means no screen description is needed. The PaLM-CoT and BC results are from Rawles et al. (2023). The GPT-4V result is from Yan et al. (2023). The other results are based on our own implementations. The overall score is computed as the average accuracy on all the subsets. The best average result is in **bold** face.

and is appropriate to measure the action success rate for user instructions. Besides the overall matching score, we will also compare the click region accuracy, scroll direction accuracy, action type accuracy, and typed text accuracy for a more comprehensive reference (Section 5.1).

The evaluation criteria above apply to the BC baselines and our Auto-GUI. For the LLMs, they can only click on detected GUI elements, rather than clicking at arbitrary locations. Therefore, we consider if the clicked GUI element is matched for click actions instead of comparing dual-point gestures for LLMs.

### 4.4 Implementation Details

We adopt the encoder-decoder architecture (Raffel et al., 2020) under small (60M), base (200M) and large (700M) settings in our framework. We apply FLAN-Alpaca to initialize our model weights.[1] The vision features are obtained by the frozen BLIP-2 encoder (Li et al., 2023) (version: blip2_t5_instruct). We fine-tune the models up to 10 epochs, with a learning rate of 1e-4. The maximum input sequence length is 512. The batch size is 4. Our experiments are run on 8 NVIDIA Tesla V100 32G GPUs. Training the large and base models takes 75 and 25 hours, respectively.

We develop two kinds of approaches to analyze their generalization abilities, namely Auto-GUI$_{\text{separate}}$, and Auto-GUI$_{\text{unified}}$. Specifically, Auto-GUI$_{\text{separate}}$ is trained and evaluated independently on each subset. Auto-GUI$_{\text{unified}}$ is a unified model trained on the training sets of each subset and evaluated on each test set. As the GoogleApps subset is 10-100 times larger than the other subsets, using all the training data to train a unified model would suffer from the data imbalance issue (Zhang et al., 2022). Therefore, we only use 10% training data of GoogleApps. At the same time, the overall computation cost can also be saved by 80%. We use Auto-GUI$_{\text{unified}}$ as the default model for analysis unless otherwise stated.

| Model | Accuracy |
|---|---|
| Auto-GUI | **74.27** |
| w/o chain of actions | 68.53 |
| w/ previous action history | 73.78 |
| w/ future action plan | 68.81 |
| w/o coordinate normalization | 70.23 |

Table 2: Ablation study of Auto-GUI.

### 4.5 Main Results

Table 1 shows the main results. Based on the results, we have the following observations.

(i) Auto-GUI$_{\text{unified}}$ achieves the best overall performance compared with all the baselines. Compared with separate (not unified) models, Auto-GUI$_{\text{unified}}$ shows general effectiveness across various tasks. The results show that a unified multimodal model out of *first principles thinking* can serve as a strong autonomous agent. Compared with previous BC models, Auto-GUI$_{\text{unified}}$ has two major advantages. First, Auto-GUI$_{\text{unified}}$ is a unified model that can be adapted to different scenarios without the need to train specific models for each task. Second, Auto-GUI$_{\text{unified}}$ does not need additional annotations and is more practical in real-world applications. Furthermore, Auto-GUI yields divergent performance across subsets. We provide the explanation in Appendix C.1 to save space.

[1] https://github.com/declare-lab/flan-alpaca.

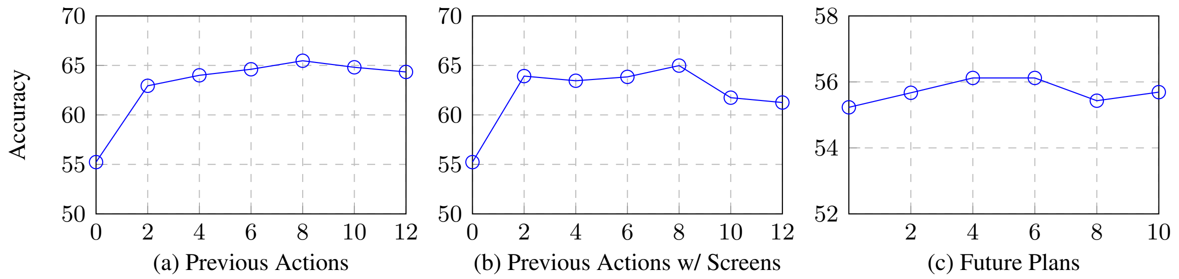

(a) Previous Actions (b) Previous Actions w/ Screens (c) Future Plans

Figure 3: Performance of Auto-GUI with respect to varying numbers of chains of actions.

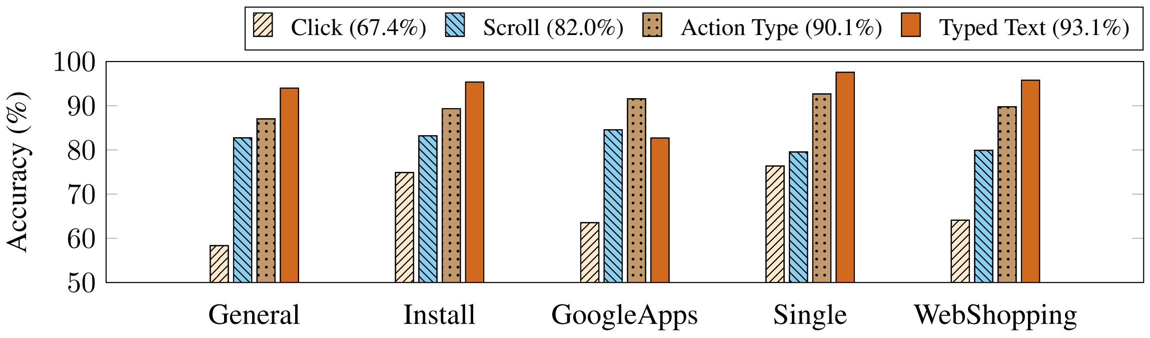

Figure 4: Category accuracy of Auto-GUI. Values in parentheses represent the average accuracy on the subsets.

(ii) Both the chain of actions and coordinate normalization contribute to the overall performance (+5.74% and 4.04%, respectively), as evidenced by the ablation study in Table 2. Additionally, we set the maximum numbers of the previous actions and future actions to 8 and 4, respectively. The choice is made according to our analysis of the General subset with Auto-GUI$_{\text{separate}}$ (Figure 3). The model under those setups achieves the optimal performance, and neither the input nor output sequence lengths exceed the model limit.

(iii) For the LLMs, using either prompting or fine-tuning techniques does not achieve competitive performance compared with multimodal approaches. The most plausible reason is that they learn from the parsed HTML elements of the screen so that they may suffer from information loss compared with more informative vision features of the screens. Specifically, we find that ChatGPT is quite accurate at predicting the action type but fails at lower-level executions (Appendix C.4).

## 5 Analysis

### 5.1 Category accuracy

To dive into the capability of Auto-GUI, we calculate the click region accuracy, scroll direction accuracy, action type accuracy, and typed text accuracy. Figure 4 presents the results. We see that Auto-GUI achieves over 90% action type accuracy on average. In contrast, the major challenges lie within the click region and scroll direction predictions. Although the model is able to predict the right action most of the time, it tends to click a wrong place or scroll in a wrong direction. The result reveals a future direction of improving the model's ability to understand the screen layouts, e.g., using more advanced vision features.

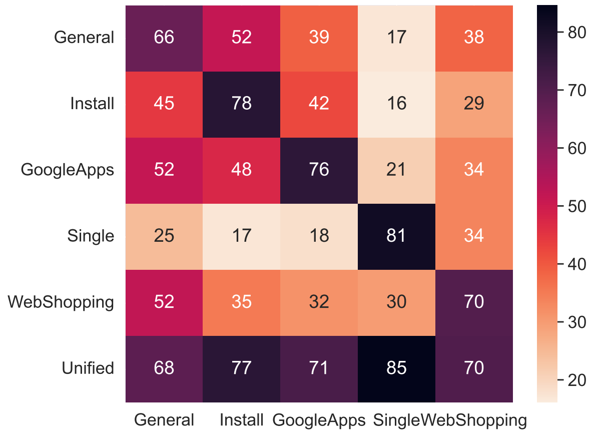

| | General | Install | GoogleApps | Single | WebShopping |
|---|---|---|---|---|---|
| General | 66 | 52 | 39 | 17 | 38 |
| Install | 45 | 78 | 42 | 16 | 29 |
| GoogleApps | 52 | 48 | 76 | 21 | 34 |
| Single | 25 | 17 | 18 | 81 | 34 |
| WebShopping | 52 | 35 | 32 | 30 | 70 |
| Unified | 68 | 77 | 71 | 85 | 70 |

Figure 5: Dataset transfer results of Auto-GUI.

### 5.2 Generalization Ability

As our approach is designed under first principles thinking and does not rely on pre-defined internal APIs, it could be easily generalized to new task domains. To verify the generality, we evaluate the performance of Auto-GUI$_{\text{separate}}$ on each subset in Figure 5. For example, we train an Auto-GUI$_{\text{separate}}$ model on the training set of General and then test its performance on the tests of each subset.

| Model | Overall | General | Install | GoogleApps | Single | WebShopping |
|---|---|---|---|---|---|---|
| Auto-GUI on CLIP | 71.84 | 66.28 | 74.40 | 69.71 | 81.60 | 67.23 |
| Auto-GUI on BLIP-2 | 74.27 | 68.24 | 76.89 | 71.37 | 84.58 | 70.26 |
| Auto-GUI on Vanilla-T5$_{\text{large}}$ | 72.98 | 66.61 | 75.40 | 70.86 | 83.47 | 68.54 |
| Auto-GUI on FLAN-T5$_{\text{large}}$ | 73.36 | 67.59 | 76.35 | 70.71 | 83.01 | 69.12 |
| Auto-GUI on FLAN-Alpaca$_{\text{large}}$ | 74.27 | 68.24 | 76.89 | 71.37 | 84.58 | 70.26 |
| Auto-GUI on FLAN-Alpaca$_{\text{small}}$ | 71.38 | 65.26 | 74.90 | 68.70 | 81.20 | 66.83 |
| Auto-GUI on FLAN-Alpaca$_{\text{base}}$ | 72.84 | 66.97 | 75.93 | 70.29 | 82.56 | 68.46 |
| Auto-GUI on FLAN-Alpaca$_{\text{large}}$ | 74.27 | 68.24 | 76.89 | 71.37 | 84.58 | 70.26 |

Table 3: Results varying vision features and pre-trained language model weights.

| Model | Feature Extraction (s/n) | Model Inference (s/n) | Peak GPU Memory (GB) |
|---|---|---|---|
| Auto-GUI$_{\text{base}}$ | 0.06 | 0.19 (45x) | 4.6 (10x) |
| Auto-GUI$_{\text{large}}$ | 0.06 | 0.59 (15x) | 8.2 (6x) |
| Llama 2 | - | 8.5 | 49.7 |

Table 4: Computation cost of Auto-GUI and Llama. "s/n" is computed by time (s) divided by the number of inferences (n). Llama 2 is hosted with 8-bit quantization and float16 precision to improve the inference speed.

We see that our approach is able to achieve a decent performance, though the domains vary. This result reveals that the model could capture general knowledge for the GUI control task; thus is applicable to different domains. In addition, the unified model Auto-GUI$_{\text{unified}}$ can serve as a potential choice in real-world applications owing to more coverage of training data.

### 5.3 Comprehensive Analysis

Here, we present a comprehensive analysis of the choice of pre-trained features and model scale. The results are summarized in Table 3.

• Pre-trained Features. There are two kinds of pre-trained features used in this work, the vision features and language model weights. For vision features, we compare two popular types, CLIP (Radford et al., 2021) and BLIP-2 (Li et al., 2023). We observe that BLIP-2 achieves relatively better performance. Therefore, we use BLIP-2 by default in Auto-GUI. For pre-trained language model weights, we compare initializing the model with the vanilla T5 (Raffel et al., 2020), FLAN-T5 (Chung et al., 2022), and FLAN-Alpaca (Taori et al., 2023a) weights under the large size. We see that FLAN-Alpaca achieves the best performance as it has been optimized with Stanford Alpaca synthetic instruction tuning data.

• Model Scale. Compared with the performance gains from our technique components (chain of actions and coordinate normalization) in Table 2, the benefit of scaling parameter size becomes relatively marginal. As we observe that a larger model size does not lead to dramatic improvement in performance, we do not scale the model scale but focus on the base (220M) and large (770M) models in this work. In addition, our choice is also based on other considerations, including the constriction of GPU memory and computation budget.

### 5.4 Computation Cost

Table 4 compares the inference speed and GPU memory cost for Auto-GUI and Llama 2. Auto-GUI is able to achieve nearly real-time inference (within less than one second for an action prediction) with less than 10GB GPU memory. The inference speed is over 10 times faster than Llama 2. Our work shows the strength of the medium-sized language model in building autonomous agents, which is able to achieve competitive performance with fast inference speed and modest resource cost.

## 6 Conclusion

This work presents an autonomous GUI agent called Auto-GUI that can interact in a multimodal GUI environment without environment parsing or application-dependent API access. In addition, we propose a chain-of-action technique that leverages the previously executed actions and future action plans to help the agent decide what action to execute. Experimental results show that Auto-GUI achieves superior performance to previous prompting-based and fine-tuning baselines, verifying that a unified multimodal model out of first principles thinking can serve as a strong autonomous agent. Besides the strong performance and generality across domains, Auto-GUI infers as fast as within less than one second.

## Limitations

We acknowledge two primary limitations in our study. First, we opted not to extend the approach to extremely large models because our work aims to provide a simple yet effective solution for autonomous GUI agents. Besides, our empirical results indicate that increasing model sizes does not result in significant performance gains for the task. Second, our experiments and analysis were exclusively conducted on AITW, which is the largest-scale and widely recognized benchmark dataset in the research line of autonomous GUI agents, to provide timely and pertinent insights. Given the rapid development of the field, we anticipate future studies to explore the application of our approach on other benchmark datasets as they become available.

## References

Adept. 2022. Act-1: Transformer for actions. https://www.adept.ai/act.

Aristotle. Physics 184a10–21.

Tom B. Brown, Benjamin Mann, Nick Ryder, Melanie Subbiah, Jared Kaplan, Prafulla Dhariwal, Arvind Neelakantan, Pranav Shyam, Girish Sastry, Amanda Askell, Sandhini Agarwal, Ariel Herbert-Voss, Gretchen Krueger, Tom Henighan, Rewon Child, Aditya Ramesh, Daniel M. Ziegler, Jeffrey Wu, Clemens Winter, Christopher Hesse, Mark Chen, Eric Sigler, Mateusz Litwin, Scott Gray, Benjamin Chess, Jack Clark, Christopher Berner, Sam McCandlish, Alec Radford, Ilya Sutskever, and Dario Amodei. 2020. Language models are few-shot learners. In *Advances in Neural Information Processing Systems 33: Annual Conference on Neural Information Processing Systems 2020, NeurIPS 2020, December 6-12, 2020, virtual*.

Kanzhi Cheng, Qiushi Sun, Yougang Chu, Fangzhi Xu, Yantao Li, Jianbing Zhang, and Zhiyong Wu. 2024. Seeclick: Harnessing gui grounding for advanced visual gui agents. *ArXiv preprint*, abs/2401.10935.

Wei-Lin Chiang, Zhuohan Li, Zi Lin, Ying Sheng, Zhanghao Wu, Hao Zhang, Lianmin Zheng, Siyuan Zhuang, Yonghao Zhuang, Joseph E Gonzalez, et al. 2023. Vicuna: An open-source chatbot impressing gpt-4 with 90%* chatgpt quality. https://vicuna.lmsys.org.

Aakanksha Chowdhery, Sharan Narang, Jacob Devlin, Maarten Bosma, Gaurav Mishra, Adam Roberts, Paul Barham, Hyung Won Chung, Charles Sutton, Sebastian Gehrmann, et al. 2022. Palm: Scaling language modeling with pathways. *ArXiv preprint*, abs/2204.02311.

Hyung Won Chung, Le Hou, Shayne Longpre, Barret Zoph, Yi Tay, William Fedus, Eric Li, Xuezhi Wang, Mostafa Dehghani, Siddhartha Brahma, et al. 2022. Scaling instruction-finetuned language models. *ArXiv preprint*, abs/2210.11416.

Difei Gao, Lei Ji, Zechen Bai, Mingyu Ouyang, Peiran Li, Dongxing Mao, Qinchen Wu, Weichen Zhang, Peiyi Wang, Xiangwu Guo, et al. 2023. Assistgui: Task-oriented desktop graphical user interface automation. *ArXiv preprint*, abs/2312.13108.

Izzeddin Gur, Hiroki Furuta, Austin Huang, Mustafa Safdari, Yutaka Matsuo, Douglas Eck, and Aleksandra Faust. 2023. A real-world webagent with planning, long context understanding, and program synthesis. *ArXiv preprint*, abs/2307.12856.

James Hendler. 1999. Is there an intelligent agent in your future? *Nature*, 11.

Sirui Hong, Xiawu Zheng, Jonathan Chen, Yuheng Cheng, Jinlin Wang, Ceyao Zhang, Zili Wang, Steven Ka Shing Yau, Zijuan Lin, Liyang Zhou, Chenyu Ran, Lingfeng Xiao, and Chenglin Wu. 2023a. Metagpt: Meta programming for multi-agent collaborative framework.

Wenyi Hong, Weihan Wang, Qingsong Lv, Jiazheng Xu, Wenmeng Yu, Junhui Ji, Yan Wang, Zihan Wang, Yuxiao Dong, Ming Ding, et al. 2023b. Cogagent: A visual language model for gui agents. *ArXiv preprint*, abs/2312.08914.

Terence Irwin. 1989. *Aristotle's first principles*. Clarendon Press.

Jing Yu Koh, Robert Lo, Lawrence Jang, Vikram Duvvur, Ming Chong Lim, Po-Yu Huang, Graham Neubig, Shuyan Zhou, Ruslan Salakhutdinov, and Daniel Fried. 2024. Visualwebarena: Evaluating multimodal agents on realistic visual web tasks. *ArXiv preprint*, abs/2401.13649.

Takeshi Kojima, Shixiang Shane Gu, Machel Reid, Yutaka Matsuo, and Yusuke Iwasawa. 2022. Large language models are zero-shot reasoners. *ArXiv preprint*, abs/2205.11916.

Junnan Li, Dongxu Li, Silvio Savarese, and Steven Hoi. 2023. Blip-2: Bootstrapping language-image pretraining with frozen image encoders and large language models. *ArXiv preprint*, abs/2301.12597.

Xiao Liu, Hao Yu, Hanchen Zhang, Yifan Xu, Xuanyu Lei, Hanyu Lai, Yu Gu, Hangliang Ding, Kaiwen Men, Kejuan Yang, et al. 2023. Agentbench: Evaluating llms as agents. *ArXiv preprint*, abs/2308.03688.

Pattie Maes. 1995. Agents that reduce work and information overload. In *Readings in human–computer interaction*, pages 811–821. Elsevier.

Yohei Nakajima. 2023. Babyagi. https://github.com/yoheinakajima/babyagi.

Maxwell Nye, Anders Johan Andreassen, Guy Gur-Ari, Henryk Michalewski, Jacob Austin, David Bieber, David Dohan, Aitor Lewkowycz, Maarten Bosma, David Luan, et al. 2022. Show your work: Scratchpads for intermediate computation with language models. In *Deep Learning for Code Workshop*.

OpenAI. 2023. Gpt-4 technical report.

Joon Sung Park, Joseph C O'Brien, Carrie J Cai, Meredith Ringel Morris, Percy Liang, and Michael S Bernstein. 2023. Generative agents: Interactive simulacra of human behavior. *ArXiv preprint*, abs/2304.03442.

Alec Radford, Jong Wook Kim, Chris Hallacy, Aditya Ramesh, Gabriel Goh, Sandhini Agarwal, Girish Sastry, Amanda Askell, Pamela Mishkin, Jack Clark, Gretchen Krueger, and Ilya Sutskever. 2021. Learning transferable visual models from natural language supervision. In *Proceedings of the 38th International Conference on Machine Learning, ICML 2021, 18-24 July 2021, Virtual Event*, volume 139 of *Proceedings of Machine Learning Research*, pages 8748–8763. PMLR.

Colin Raffel, Noam Shazeer, Adam Roberts, Katherine Lee, Sharan Narang, Michael Matena, Yanqi Zhou, Wei Li, and Peter J. Liu. 2020. Exploring the limits of transfer learning with a unified text-to-text transformer. *J. Mach. Learn. Res.*, 21:140:1–140:67.

Christopher Rawles, Alice Li, Daniel Rodriguez, Oriana Riva, and Timothy P Lillicrap. 2023. Androidinthewild: A large-scale dataset for android device control. In *Thirty-seventh Conference on Neural Information Processing Systems Datasets and Benchmarks Track*.

Reworkd. 2023. Agentgpt. https://github.com/reworkd/AgentGPT.

Toran Bruce Richards. 2023. Auto-gpt: An autonomous gpt-4 experiment. https://github.com/Significant-Gravitas/Auto-GPT.

Victor Sanh, Albert Webson, Colin Raffel, Stephen H. Bach, Lintang Sutawika, Zaid Alyafeai, Antoine Chaffin, Arnaud Stiegler, Arun Raja, Manan Dey, M Saiful Bari, Canwen Xu, Urmish Thakker, Shanya Sharma Sharma, Eliza Szczechla, Taewoon Kim, Gunjan Chhablani, Nihal V. Nayak, Debajyoti Datta, Jonathan Chang, Mike Tian-Jian Jiang, Han Wang, Matteo Manica, Sheng Shen, Zheng Xin Yong, Harshit Pandey, Rachel Bawden, Thomas Wang, Trishala Neeraj, Jos Rozen, Abheesht Sharma, Andrea Santilli, Thibault Févry, Jason Alan Fries, Ryan Teehan, Teven Le Scao, Stella Biderman, Leo Gao, Thomas Wolf, and Alexander M. Rush. 2022. Multitask prompted training enables zero-shot task generalization. In *The Tenth International Conference on Learning Representations, ICLR 2022, Virtual Event, April 25-29, 2022*. OpenReview.net.

John R Searle. 1969. *Speech acts: An essay in the philosophy of language*, volume 626. Cambridge university press.

Yunpeng Song, Yiheng Bian, Yongtao Tang, and Zhongmin Cai. 2023. Navigating interfaces with ai for enhanced user interaction. *ArXiv preprint*, abs/2312.11190.

Theodore Sumers, Shunyu Yao, Karthik Narasimhan, and Thomas L Griffiths. 2023. Cognitive architectures for language agents. *ArXiv preprint*, abs/2309.02427.

Liangtai Sun, Xingyu Chen, Lu Chen, Tianle Dai, Zichen Zhu, and Kai Yu. 2022. META-GUI: Towards multi-modal conversational agents on mobile GUI. In *Proceedings of the 2022 Conference on Empirical Methods in Natural Language Processing*, pages 6699–6712, Abu Dhabi, United Arab Emirates. Association for Computational Linguistics.

Srinivas Sunkara, Maria Wang, Lijuan Liu, Gilles Baechler, Yu-Chung Hsiao, Jindong Chen, Abhanshu Sharma, and James W. W. Stout. 2022. Towards better semantic understanding of mobile interfaces. In *Proceedings of the 29th International Conference on Computational Linguistics*, pages 5636–5650, Gyeongju, Republic of Korea. International Committee on Computational Linguistics.

Rohan Taori, Ishaan Gulrajani, Tianyi Zhang, Yann Dubois, Xuechen Li, Carlos Guestrin, Percy Liang, and Tatsunori B Hashimoto. 2023a. Alpaca: A strong, replicable instruction-following model. *Stanford Center for Research on Foundation Models. https://crfm. stanford. edu/2023/03/13/alpaca. html.*

Rohan Taori, Ishaan Gulrajani, Tianyi Zhang, Yann Dubois, Xuechen Li, Carlos Guestrin, Percy Liang, and Tatsunori B Hashimoto. 2023b. Stanford alpaca: An instruction-following llama model. https://github.com/tatsu-lab/stanford_alpaca.

Hugo Touvron, Louis Martin, Kevin Stone, Peter Albert, Amjad Almahairi, Yasmine Babaei, Nikolay Bashlykov, Soumya Batra, Prajjwal Bhargava, Shruti Bhosale, et al. 2023. Llama 2: Open foundation and fine-tuned chat models. *ArXiv preprint*, abs/2307.09288.

Ashish Vaswani, Noam Shazeer, Niki Parmar, Jakob Uszkoreit, Llion Jones, Aidan N. Gomez, Lukasz Kaiser, and Illia Polosukhin. 2017. Attention is all you need. In *Advances in Neural Information Processing Systems 30: Annual Conference on Neural Information Processing Systems 2017, December 4-9, 2017, Long Beach, CA, USA*, pages 5998–6008.

Bryan Wang, Gang Li, and Yang Li. 2023a. Enabling conversational interaction with mobile ui using large language models. In *Proceedings of the 2023 CHI Conference on Human Factors in Computing Systems*, pages 1–17.

Guanzhi Wang, Yuqi Xie, Yunfan Jiang, Ajay Mandlekar, Chaowei Xiao, Yuke Zhu, Linxi Fan, and Anima Anandkumar. 2023b. Voyager: An open-ended embodied agent with large language models. *ArXiv preprint*, abs/2305.16291.

Lei Wang, Chen Ma, Xueyang Feng, Zeyu Zhang, Hao Yang, Jingsen Zhang, Zhiyuan Chen, Jiakai Tang, Xu Chen, Yankai Lin, et al. 2023c. A survey on large language model based autonomous agents. *ArXiv preprint*, abs/2308.11432.

Jason Wei, Xuezhi Wang, Dale Schuurmans, Maarten Bosma, Ed Chi, Quoc Le, and Denny Zhou. 2022. Chain of thought prompting elicits reasoning in large language models. *ArXiv preprint*, abs/2201.11903.

Hao Wen, Yuanchun Li, Guohong Liu, Shanhui Zhao, Tao Yu, Toby Jia-Jun Li, Shiqi Jiang, Yunhao Liu, Yaqin Zhang, and Yunxin Liu. 2023. Empowering llm to use smartphone for intelligent task automation. *ArXiv preprint*, abs/2308.15272.

Michael Wooldridge and Nicholas R Jennings. 1995. Intelligent agents: Theory and practice. *The knowledge engineering review*, 10(2):115–152.

Zhiyong Wu, Lingpeng Kong, Wei Bi, Xiang Li, and Ben Kao. 2021. Good for misconceived reasons: An empirical revisiting on the need for visual context in multimodal machine translation. In *Proceedings of the 59th Annual Meeting of the Association for Computational Linguistics and the 11th International Joint Conference on Natural Language Processing (Volume 1: Long Papers)*, pages 6153–6166, Online. Association for Computational Linguistics.

An Yan, Zhengyuan Yang, Wanrong Zhu, Kevin Lin, Linjie Li, Jianfeng Wang, Jianwei Yang, Yiwu Zhong, Julian McAuley, Jianfeng Gao, et al. 2023. Gpt-4v in wonderland: Large multimodal models for zero-shot smartphone gui navigation. *ArXiv preprint*, abs/2311.07562.

Zhao Yang, Jiaxuan Liu, Yucheng Han, Xin Chen, Zebiao Huang, Bin Fu, and Gang Yu. 2023. Appagent: Multimodal agents as smartphone users. *ArXiv preprint*, abs/2312.13771.

Xiaoyi Zhang, Lilian de Greef, Amanda Swearngin, Samuel White, Kyle Murray, Lisa Yu, Qi Shan, Jeffrey Nichols, Jason Wu, Chris Fleizach, et al. 2021. Screen recognition: Creating accessibility metadata for mobile applications from pixels. In *Proceedings of the 2021 CHI Conference on Human Factors in Computing Systems*, pages 1–15.

Zhuosheng Zhang, Kehai Chen, Rui Wang, Masao Utiyama, Eiichiro Sumita, Zuchao Li, and Hai Zhao. 2020. Neural machine translation with universal visual representation. In *8th International Conference on Learning Representations, ICLR 2020, Addis Ababa, Ethiopia, April 26-30, 2020*. OpenReview.net.

Zhuosheng Zhang, Shuohang Wang, Yichong Xu, Yuwei Fang, Wenhao Yu, Yang Liu, Hai Zhao, Chenguang Zhu, and Michael Zeng. 2022. Task compass: Scaling multi-task pre-training with task prefix. In *Findings of the Association for Computational Linguistics: EMNLP 2022*, pages 5671–5685, Abu Dhabi, United Arab Emirates. Association for Computational Linguistics.

Zhuosheng Zhang, Aston Zhang, Mu Li, and Alex Smola. 2023a. Automatic chain of thought prompting in large language models. In *The Eleventh International Conference on Learning Representations*.

Zhuosheng Zhang, Aston Zhang, Mu Li, Hai Zhao, George Karypis, and Alex Smola. 2023b. Multimodal chain-of-thought reasoning in language models. *ArXiv preprint*, abs/2302.00923.

Shuyan Zhou, Frank F Xu, Hao Zhu, Xuhui Zhou, Robert Lo, Abishek Sridhar, Xianyi Cheng, Yonatan Bisk, Daniel Fried, Uri Alon, et al. 2023. Webarena: A realistic web environment for building autonomous agents. *ArXiv preprint*, abs/2307.13854.

Xizhou Zhu, Yuntao Chen, Hao Tian, Chenxin Tao, Weijie Su, Chenyu Yang, Gao Huang, Bin Li, Lewei Lu, Xiaogang Wang, et al. 2023. Ghost in the minecraft: Generally capable agents for open-world enviroments via large language models with text-based knowledge and memory. *ArXiv preprint*, abs/2305.17144.

# A Data Details

## A.1 Data Examples

We show the data examples from the AITW benchmark dataset (Rawles et al., 2023). Figures 6-9 show the examples in each subset, i.e., General, Install, GoogleApps, Single, and WebShopping. The gold actions for each screen are depicted in the illustrations for reference.

## A.2 Data Statistics

We use the AITW benchmark dataset (Rawles et al., 2023). AITW is a large-scale benchmark dataset for GUI control, which contains natural language instructions, screenshots, and actions. There are $715K$ episodes spanning $30K$ unique instructions, covering diverse multi-step tasks such as application operation, web searching, and web shopping, on over 350 Apps and websites. This dataset covers various device types and operation systems in varying screen resolutions to ensure generality. There are five subsets in the benchmark dataset: General, Install, GoogleApps, Single, and WebShopping.

(i) General contains miscellaneous tasks that need interaction with third-party Apps and websites, as well as question answering.

(ii) Install contains tasks related to installing, uninstalling, logging Apps, and App login support.

(iii) GoogleApps contains tasks about manipulating various Google applications such as Gmail, Calendar, Photos, and Settings.

(iv) Single contains atomic tasks (e.g., "upvote the post") whose preceding actions have been already completed (e.g., opening Instagram, going to home feed, looking at a post).

(v) WebShopping contains tasks related to online shopping on E-commerce websites, e.g., searching for an item, adding an item to the cart, and viewing the shopping cart.

Table 5 presents the data statistics of the AITW dataset. Each subset is split episode-wise into a training, validation, and test set (80/10/10%).

| Dataset | Episodes | Screens | Instructions |
|---|---|---|---|
| General | 9,476 | 85,413 | 545 |
| Install | 25,760 | 250,058 | 688 |
| GoogleApps | 625,542 | 4,903,601 | 306 |
| Single | 26,303 | 85,668 | 15,366 |
| WebShopping | 28,061 | 365,253 | 13,473 |

Table 5: Dataset statistics.

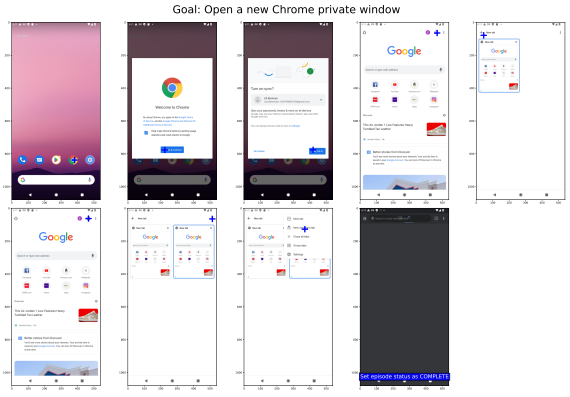
Goal: Open a new Chrome private window
Google
Set episode status as COMPLETE

Figure 6: An example episode from General.

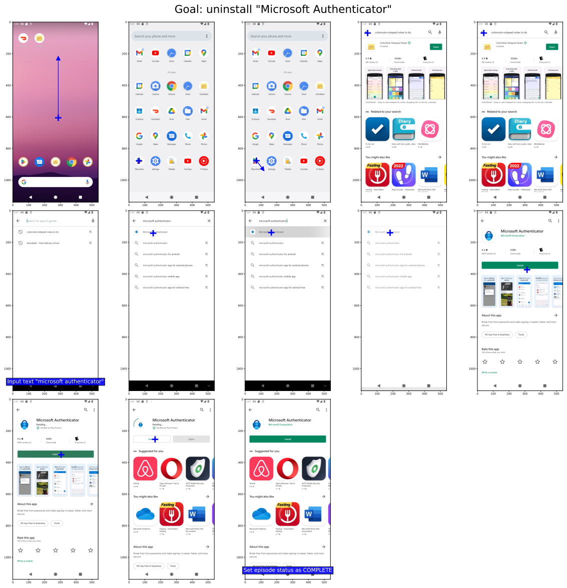
Goal: uninstall "Microsoft Authenticator"
Input text "microsoft authenticator"
Microsoft Authenticator
Set episode status as COMPLETE

Figure 7: An example episode from Install.

# B Implementation Details

## B.1 Coordinate Normalization

Recall that a target action consists of four components: action type, touch point, lift point, and typed text. We consider six action types: *dual-point gesture*, *type*, *go_back*, *go_home*, *enter*, and *status_complete*. A dual-point gesture comprises a touch point and a lift point with $[y, x]$ coordinates. The gesture actions ensure a flexible action space and can represent clicks and scrolls at arbitrary locations. For example, a gesture action {"touch_point": [0.7761, 0.7089], "lift_point": [0.7761, 0.7089]} means clicking at the coordinate [0.7761, 0.7089], while a gesture action {"touch_point": [0.1898, 0.4477], "lift_point": [0.8242, 0.4077]} means scrolling down. A type action means typing a text and the text is placed in the <typed_text> field. The other ac-

| Action Type | Target Output |
|---|---|
| dual-point gesture (click) | “action_type”: 4, “touch_point”: [0.8497, 0.5964], “lift_point”: [0.8497, 0.5964], “typed_text”: “” |
| dual-point gesture (scroll) | “action_type”: 4, “touch_point”: [0.2, 0.5], “lift_point”: [0.8, 0.5], “typed_text”: “” |
| type | “action_type”: 3, “touch_point”: [-1.0, -1.0], “lift_point”: [-1.0, -1.0], “typed_text”: “what’s the news in chile?” |
| go_back | “action_type”: 5, “touch_point”: [-1.0, -1.0], “lift_point”: [-1.0, -1.0], “typed_text”: “” |
| go_home | “action_type”: 6, “touch_point”: [-1.0, -1.0], “lift_point”: [-1.0, -1.0], “typed_text”: “” |
| enter | “action_type”: 7, “touch_point”: [-1.0, -1.0], “lift_point”: [-1.0, -1.0], “typed_text”: “” |
| status_complete | “action_type”: 10, “touch_point”: [-1.0, -1.0], “lift_point”: [-1.0, -1.0], “typed_text”: “” |

Table 6: Target output examples after the coordinate normalization.

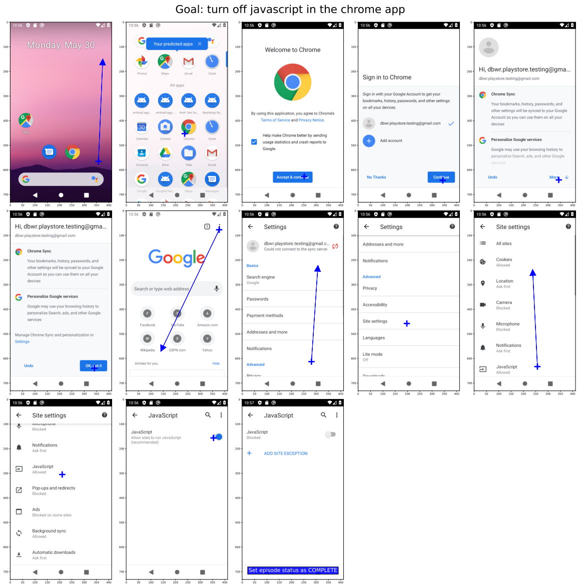
Goal: turn off javascript in the chrome app
Set episode status as COMPLETE

Figure 8: An example episode from GoogleApps.

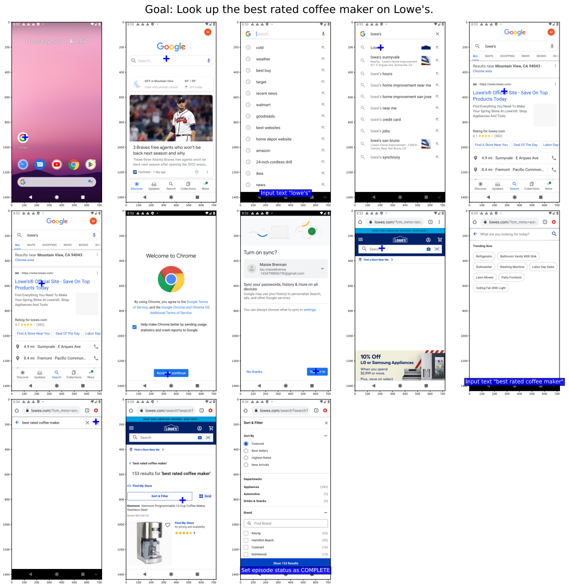
Goal: Look up the best rated coffee maker on Lowe's.
Input text "lowe's"
Input text "best rated coffee maker"
Set episode status as COMPLETE

Figure 9: An example episode from WebShopping.

tion types, i.e., go_back, go_home, enter, and status_complete are system actions, whose corresponding <touch_point>, <lift_point> fields are filled with -1, and the <typed_text> is empty.

We observe that high-precision coordinates are not necessary for representing a click or scroll action. Therefore, we apply normalized values of the coordinates, which helps accelerate convergence and mitigate the ambiguity of coordinates. The normalization is applied to click and scroll actions. For click actions, we keep four decimal places. For scroll actions, we first determine the scroll direction with the touch and lift points. Then, we transform the touch and lift points into fixed directional coordinates as follows: “up”: {[0.8, 0.5], [0.2, 0.5]}, “down”: {[0.2, 0.5], [0.8, 0.5]}, “left”: {[0.5, 0.8], [0.5, 0.2]}, “right”: {[0.5, 0.2], [0.5, 0.8]}, where {[·], [·]} consists of the touch point and lift point in the first [·] and second [·]. We provide examples of target actions in Table 6.

## B.2 Baselines

We adopt three types of baselines for comparisons. The baselines encompass the in-context earning (ICL) and fine-tuning paradigms, along with various backbone models of different sizes. This choice of baselines allows for a comprehensive comparison with our proposed approach.

(i) In-context Learning LLMs. Few-shot PaLM 2, ChatGPT (turbo-3.5) are adopted. Following previous studies (Rawles et al., 2023; Wang et al., 2023a), we feed the LLM a textual description of the screen and a user instruction. The textual description of the screen is formatted as an HTML

| Model | Overall | General | Install | GoogleApps | Single | WebShopping |
|---|---|---|---|---|---|---|
| Auto-GUI | **74.27** | **68.24** | **76.89** | **71.37** | **84.58** | **70.26** |
| w/o chain of actions | 68.53 | 58.99 | 72.06 | 67.50 | 81.25 | 62.86 |
| w/ previous action history | 73.78 | 67.97 | 76.66 | 71.00 | 83.64 | 69.62 |
| w/ future action plan | 68.81 | 59.01 | 72.34 | 67.95 | 81.53 | 63.24 |
| w/o coordinate normalization | 70.23 | 63.79 | 73.28 | 66.63 | 82.11 | 65.33 |

Table 7: Ablation study of Auto-GUI design components. We adopt Auto-GUI$_{\text{unified}}$ for analysis.

| Model | Overall | General | Install | GoogleApps | Single | WebShopping |
|---|---|---|---|---|---|---|
| Auto-GUI$_{\text{base}}$ | 72.84 | 66.97 | 75.93 | 70.29 | 82.56 | 68.46 |
| w/ Screen Descriptions | 75.54 | 70.30 | 78.05 | 73.04 | 85.31 | 71.00 |

Table 8: Results of Auto-GUI when using annotated screen descriptions.

syntax, providing the information of GUI elements derived from OCR detection and icon detection from external tools (Rawles et al., 2023). The model is required to predict an action among predefined actions. If the action is clicking, the model will be required to provide the index of the clicked GUI element. Alternatively, the model needs to provide the scroll direction if the action is scrolling. In addition, 5-shot CoT prompting is leveraged to improve the performance (Appendix B.3). In addition, we report the results of the multimodal GPT-4V by taking the vision image and action history as the input based on Yan et al. (2023).

(ii) Fine-tuned LLMs. We adopt Llama 2 (Touvron et al., 2023) as the baseline and fine-tune it with LoRA. We feed the model with the user instruction and the screen descriptions in HTML syntax (the same as adopted for in-context learning LLMs). The model is expected to predict the action in the same output format as in-context learning LLMs. As fine-tuning an LLM is expensive, we randomly sample 1% training data to help the LLM adapt to our tasks.

(iii) Specialized GUI Agent. We adopted the Behavioural Cloning (BC) agent, which reported the state-of-the-art performance in Rawles et al. (2023). BC is a Transformer-based architecture that takes a task instruction, the current screen, and a stacked history of screen observations and actions as input. The task instruction and OCR-detected texts are encoded by a pre-trained BERT. The icons are represented by the embeddings for each of the bounding box points. The screen history is modeled by the $\{x, y\}$ positions of the touch and lift actions. All the embedded representations are fused to predict the action by a decoder. There are two BC variants, BC-single and BC-history, depending on whether the model takes as input the screen-action history.

### B.3 LLM Prompt

We use the prompt in Figures 10-11 for PaLM 2-CoT and ChatGPT-CoT owing to its optimal performance reported in Rawles et al. (2023).

## C Further Analysis

### C.1 Subset Analysis

We notice that Auto-GUI$_{\text{unified}}$ performs relatively inferior to BC-history on the two App-centered subsets, Install and GoogleApps. It is reasonable because we only use 10% training data of GoogleApps considering the data balance and computation overhead. We observe that the performance does not improve when we use all the training data of GoogleApps, possibly due to the data imbalance issue (Zhang et al., 2022). In contrast, our separate model Auto-GUI$_{\text{separate}}$ can achieve better performance than BC-history, showing that our approach is better than BC-history under the same training setting. As we aim to study a simple and unified approach that achieves generally strong performance, we leave the treatment of the data imbalance issue in future work.

### C.2 Ablation Study

Table 7 shows the detailed results of the ablation study. We see that both the chain of actions and coordinate normalization contribute to the overall performance (+5.74% and 4.04%, respectively).

### C.3 Using Screen Descriptions

We are interested in whether Auto-GUI can be further improved when screen annotations are available. Therefore, we incorporate screen descriptions containing icon and text information, organized in HTML syntax, into our language input $X_{\text{language}}$. Detailed examples of screen descriptions can be found in the "Screen" block in Appendix B.3.

In Table 8, we see that Auto-GUI can perform better when the annotated screen descriptions are available. The results show that there is still room for performance gains for Auto-GUI. However, as the annotations are not always available in real-world applications, we do not include them by default in our framework.

### C.4 Category Results with the ICL Baseline

To understand how the ICL baseline performs on our task and assess the advantage of Auto-GUI, we conduct a category comparison with ChatGPT.

| Model | Overall | Action Type | Click | Scroll |
|---|---|---|---|---|
| ChatGPT | 5.93 | 41.72 | 8.50 | 4.00 |
| Auto-GUI | 68.24 | 87.03 | 58.34 | 82.74 |

Table 9: Category comparison with the ICL baseline on the General test set.

In Table 9, we see that the ICL method (ChatGPT) is quite accurate at predicting the action type (41.72%) but fails at lower-level executions, e.g., clicking positions (8.5%) and scrolling directions (4.0%). The results show that using HTML-based layout information is not enough to accurately execute actions. In contrast, Auto-GUI has the advantage of predicting both action types and performing low-level executions by leveraging multimodal perception and the chain-of-action technique.

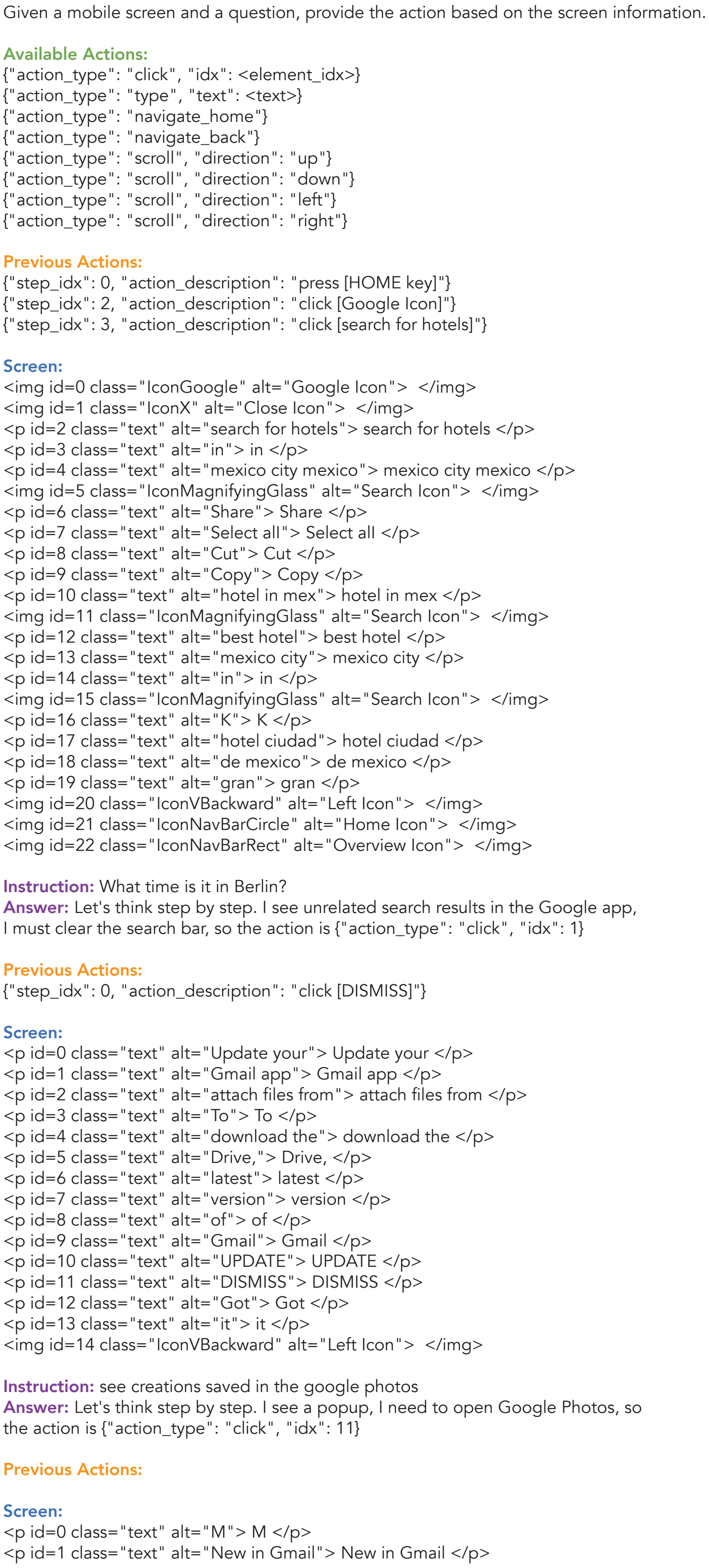

```
Given a mobile screen and a question, provide the action based on the screen information.

Available Actions:
{"action_type": "click", "idx": <element_idx>}
{"action_type": "type", "text": <text>}
{"action_type": "navigate_home"}
{"action_type": "navigate_back"}
{"action_type": "scroll", "direction": "up"}
{"action_type": "scroll", "direction": "down"}
{"action_type": "scroll", "direction": "left"}
{"action_type": "scroll", "direction": "right"}

Previous Actions:
{"step_idx": 0, "action_description": "press [HOME key]"}
{"step_idx": 2, "action_description": "click [Google Icon]"}
{"step_idx": 3, "action_description": "click [search for hotels]"}

Screen:
<img id=0 class="IconGoogle" alt="Google Icon">  </img>
<img id=1 class="IconX" alt="Close Icon">  </img>
<p id=2 class="text" alt="search for hotels"> search for hotels </p>
<p id=3 class="text" alt="in"> in </p>
<p id=4 class="text" alt="mexico city mexico"> mexico city mexico </p>
<img id=5 class="IconMagnifyingGlass" alt="Search Icon">  </img>
<p id=6 class="text" alt="Share"> Share </p>
<p id=7 class="text" alt="Select all"> Select all </p>
<p id=8 class="text" alt="Cut"> Cut </p>
<p id=9 class="text" alt="Copy"> Copy </p>
<p id=10 class="text" alt="hotel in mex"> hotel in mex </p>
<img id=11 class="IconMagnifyingGlass" alt="Search Icon">  </img>
<p id=12 class="text" alt="best hotel"> best hotel </p>
<p id=13 class="text" alt="mexico city"> mexico city </p>
<p id=14 class="text" alt="in"> in </p>
<img id=15 class="IconMagnifyingGlass" alt="Search Icon">  </img>
<p id=16 class="text" alt="K"> K </p>
<p id=17 class="text" alt="hotel ciudad"> hotel ciudad </p>
<p id=18 class="text" alt="de mexico"> de mexico </p>
<p id=19 class="text" alt="gran"> gran </p>
<img id=20 class="IconVBackward" alt="Left Icon">  </img>
<img id=21 class="IconNavBarCircle" alt="Home Icon">  </img>
<img id=22 class="IconNavBarRect" alt="Overview Icon">  </img>

Instruction: What time is it in Berlin?
Answer: Let's think step by step. I see unrelated search results in the Google app,
I must clear the search bar, so the action is {"action_type": "click", "idx": 1}

Previous Actions:
{"step_idx": 0, "action_description": "click [DISMISS]"}

Screen:
<p id=0 class="text" alt="Update your"> Update your </p>
<p id=1 class="text" alt="Gmail app"> Gmail app </p>
<p id=2 class="text" alt="attach files from"> attach files from </p>
<p id=3 class="text" alt="To"> To </p>
<p id=4 class="text" alt="download the"> download the </p>
<p id=5 class="text" alt="Drive,"> Drive, </p>
<p id=6 class="text" alt="latest"> latest </p>
<p id=7 class="text" alt="version"> version </p>
<p id=8 class="text" alt="of"> of </p>
<p id=9 class="text" alt="Gmail"> Gmail </p>
<p id=10 class="text" alt="UPDATE"> UPDATE </p>
<p id=11 class="text" alt="DISMISS"> DISMISS </p>
<p id=12 class="text" alt="Got"> Got </p>
<p id=13 class="text" alt="it"> it </p>
<img id=14 class="IconVBackward" alt="Left Icon">  </img>

Instruction: see creations saved in the google photos
Answer: Let's think step by step. I see a popup, I need to open Google Photos, so
the action is {"action_type": "click", "idx": 11}

Previous Actions:

Screen:
<p id=0 class="text" alt="M"> M </p>
<p id=1 class="text" alt="New in Gmail"> New in Gmail </p>
```

Figure 10: LLM Prompt (Part-I).

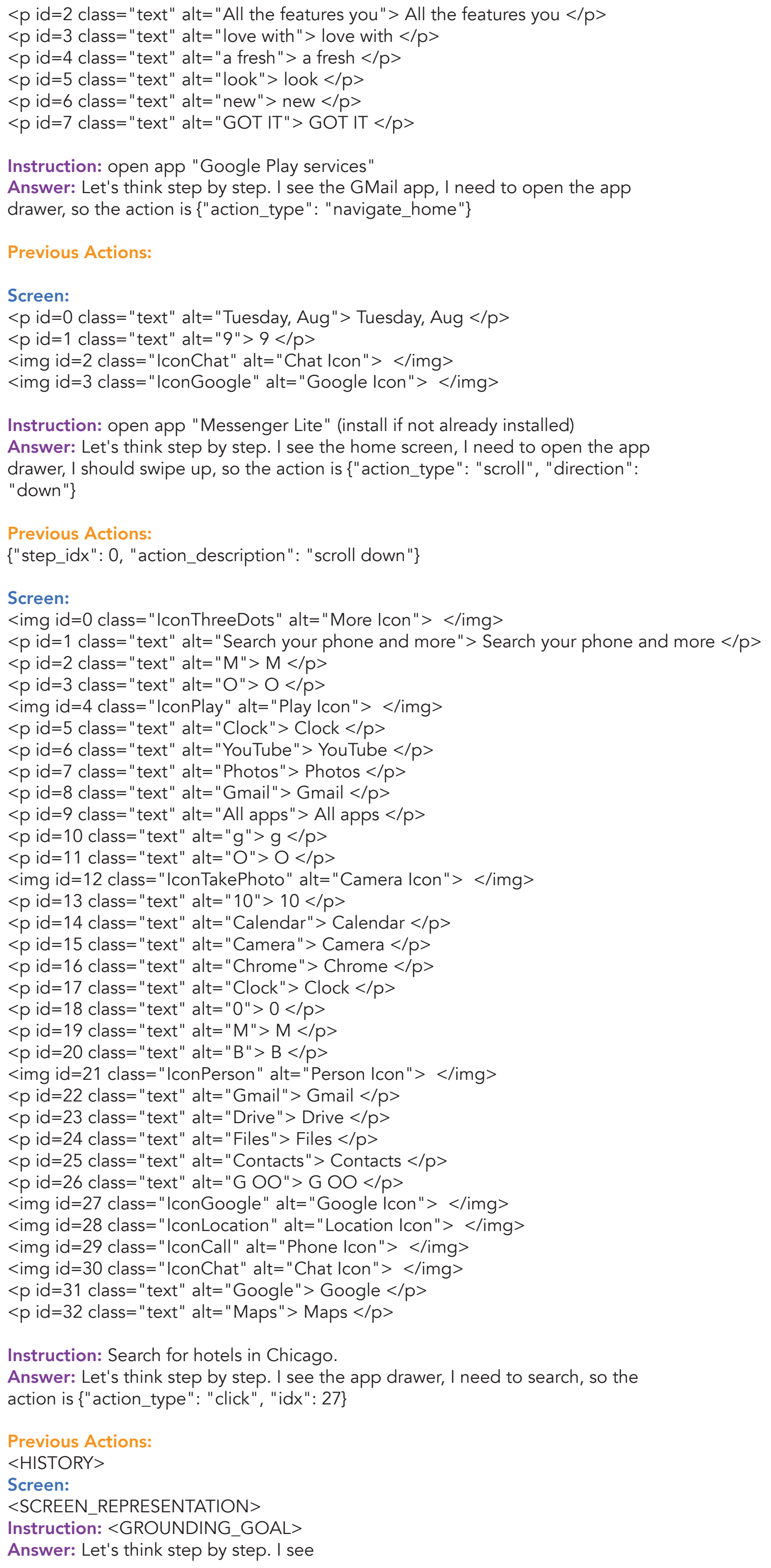

```
<p id=2 class="text" alt="All the features you"> All the features you </p>
<p id=3 class="text" alt="love with"> love with </p>
<p id=4 class="text" alt="a fresh"> a fresh </p>
<p id=5 class="text" alt="look"> look </p>
<p id=6 class="text" alt="new"> new </p>
<p id=7 class="text" alt="GOT IT"> GOT IT </p>

Instruction: open app "Google Play services"
Answer: Let's think step by step. I see the GMail app, I need to open the app
drawer, so the action is {"action_type": "navigate_home"}

Previous Actions:

Screen:
<p id=0 class="text" alt="Tuesday, Aug"> Tuesday, Aug </p>
<p id=1 class="text" alt="9"> 9 </p>
<img id=2 class="IconChat" alt="Chat Icon">  </img>
<img id=3 class="IconGoogle" alt="Google Icon">  </img>

Instruction: open app "Messenger Lite" (install if not already installed)
Answer: Let's think step by step. I see the home screen, I need to open the app
drawer, I should swipe up, so the action is {"action_type": "scroll", "direction":
"down"}

Previous Actions:
{"step_idx": 0, "action_description": "scroll down"}

Screen:
<img id=0 class="IconThreeDots" alt="More Icon">  </img>
<p id=1 class="text" alt="Search your phone and more"> Search your phone and more </p>
<p id=2 class="text" alt="M"> M </p>
<p id=3 class="text" alt="O"> O </p>
<img id=4 class="IconPlay" alt="Play Icon">  </img>
<p id=5 class="text" alt="Clock"> Clock </p>
<p id=6 class="text" alt="YouTube"> YouTube </p>
<p id=7 class="text" alt="Photos"> Photos </p>
<p id=8 class="text" alt="Gmail"> Gmail </p>
<p id=9 class="text" alt="All apps"> All apps </p>
<p id=10 class="text" alt="g"> g </p>
<p id=11 class="text" alt="O"> O </p>
<img id=12 class="IconTakePhoto" alt="Camera Icon">  </img>
<p id=13 class="text" alt="10"> 10 </p>
<p id=14 class="text" alt="Calendar"> Calendar </p>
<p id=15 class="text" alt="Camera"> Camera </p>
<p id=16 class="text" alt="Chrome"> Chrome </p>
<p id=17 class="text" alt="Clock"> Clock </p>
<p id=18 class="text" alt="0"> 0 </p>
<p id=19 class="text" alt="M"> M </p>
<p id=20 class="text" alt="B"> B </p>
<img id=21 class="IconPerson" alt="Person Icon">  </img>
<p id=22 class="text" alt="Gmail"> Gmail </p>
<p id=23 class="text" alt="Drive"> Drive </p>
<p id=24 class="text" alt="Files"> Files </p>
<p id=25 class="text" alt="Contacts"> Contacts </p>
<p id=26 class="text" alt="G OO"> G OO </p>
<img id=27 class="IconGoogle" alt="Google Icon">  </img>
<img id=28 class="IconLocation" alt="Location Icon">  </img>
<img id=29 class="IconCall" alt="Phone Icon">  </img>
<img id=30 class="IconChat" alt="Chat Icon">  </img>
<p id=31 class="text" alt="Google"> Google </p>
<p id=32 class="text" alt="Maps"> Maps </p>

Instruction: Search for hotels in Chicago.
Answer: Let's think step by step. I see the app drawer, I need to search, so the
action is {"action_type": "click", "idx": 27}

Previous Actions:
<HISTORY>
Screen:
<SCREEN_REPRESENTATION>
Instruction: <GROUNDING_GOAL>
Answer: Let's think step by step. I see
```

Figure 11: LLM Prompt (Part-II).